Forest Biomass Estimation at High Spatial Resolution: Radar Versus Lidar Sensors

Mihai A. Tanase, Rocco Panciera, Kim Lowell, Cristina Aponte, Jorg M. Hacker, and Jeffrey P. Walker

***Abstract*—This letter evaluates the biomass-retrieval error in pine-dominated stands when using high-spatial-resolution airborne measurements from fully polarimetric L-band radar and airborne laser scanning sensors. Information on total above–ground biomass was estimated through allometric relationships from plot-level field measurements. Multiple-linear-regression models were developed to model relationships between biomass and radar/lidar data. Overall, lidar data provided lower estimation errors (17.2 $\mathbf{t \cdot ha^{-1}}$, 28% relative) when compared with radar data (30.3 $\mathbf{t \cdot ha^{-1}}$, 61% relative). However, for the 30–100 $\mathbf{t \cdot ha^{-1}}$ biomass range, the relative error from radar-based models was only 9% higher than that from lidar-based models. This suggests that high-spatial-resolution radar data could provide fundamentally similar results to lidar for some biomass intervals. This is an important finding for large-scale biomass estimation that needs to rely upon satellite data, as there are no lidar satellites planned for the foreseeable future.**

***Index Terms*—Biomass, L-band radar, small-footprint lidar.**

I. Introduction

RETRIEVAL of forest characteristics is one of the main research topics of the remote-sensing community. Analysis of changes in forest cover and carbon stocks is of major interest for many agencies that address environmental, economic, and legal issues. The last two decades were mostly focused on the extraction of biomass information from synthetic aperture radar (SAR) and light detection and ranging (lidar) sensors. The first relationships between forest biomass and SAR backscatter coefficients were demonstrated more than three decades ago. Lidar research on forest biomass retrieval started at about the same time, but during the last decade, it has become the method of choice for the retrieval of forest characteristics for management purposes, following the development of commercially viable airborne systems. Results from numerous studies conducted using both small and large footprint lidar sensors demonstrated their high accuracy when retrieving forest biomass [1], [2], with relatively larger errors obtained when using SAR data [3]–[5], due to signal saturation and related environmental conditions. Although many studies have assessed the accuracy of forest biomass retrieval from each of these sensor types, only few have specifically compared lidar and radar backscatter for biomass estimation and evaluated the eventual synergies between the two sensor types [6]–[8], with a fourth study [9] analyzing only radar interferometric heights. None of these studies analyzed L-band radar data or took advantage of a fully polarimetric sensor. In addition, most previous studies did not have concurrent field and/or remotely sensed data acquisitions (i.e., time lags varied from six months to three years). Not knowing trees' condition (i.e., dead/live) when acquiring radar data could impact biomass/radar relationships since backscatter response for dead trees reduces significantly (i.e., shedding leaves and branches and decreasing water content—drying) especially at low frequencies such as L-band. Long time lags between lidar and radar acquisitions could also result in differentiated backscatter response solely due to changes in soil/vegetation water content for both sensor types. This study expands the current knowledge by using simultaneously acquired field and remote-sensing data (i.e., lidar and radar) of comparable spatial resolutions to specifically evaluate biomass retrieval from each sensor type and their eventual synergy. In addition, this study was carried out for forests with average biomass levels well below L-band radar saturation point (i.e., 100 $t \cdot ha^{-1}$, [10]), and the retrieval precision was given by biomass intervals.

A fully polarimetric L-band SAR and a small-footprint lidar sensor were flown within days of each other over the same forest area, with coincident ground data. Comparisons were made between the two airborne systems using extensive ground validation data. Specifically, we showed that lidar data provided the lowest biomass-retrieval error when compared with ground-based estimates and that jointly using lidar and radar data did not decrease the biomass estimation error (i.e., none of the radar-based metrics significantly improved the model performance). Nevertheless, for some biomass intervals, the estimation errors obtained using high-resolution L-band radar were similar when compared with the small-footprint lidar sensor.

II. Study Area and Data Sets

The 1800-ha Gillenbah forest study area is located in New South Wales, Australia. The vegetation is dominated by white cypress pine (*Callitris glaucophylla*), with the grey box (*Eucalyptus microcarpa*) distributed throughout the forest and accounting for only 10% of the trees (Fig. 1). The topography is nearly flat with slopes less than 5° for most of the forest. Several airborne sensors were flown during the field campaign, with

Manuscript received June 7, 2013; accepted July 15, 2013. This work was supported in part by an Australian Research Council Superscience Fellowship (FS100100040), by the Cooperative Research Centre for Spatial Information, and by the SMAPEx Discovery Project (DP0984586).

M. A. Tanase, R. Panciera, and K. Lowell are with the CRC for Spatial Information, The University of Melbourne, Parkville, VIC 3010, Australia.

C. Aponte is with the Department of Forest and Ecosystem Science, The University of Melbourne, Parkville, VIC 3010, Australia.

J. M. Hacker is with the Airborne Research Australia, School of Environment, Flinders University, Salisbury South, SA 5106, Australia.

J. P. Walker is with the Department of Civil Engineering, Monash University, Clayton, VIC 3800, Australia.

Color versions of one or more of the figures in this paper are available online at http://ieeexplore.ieee.org.

Digital Object Identifier 10.1109/LGRS.2013.2276947

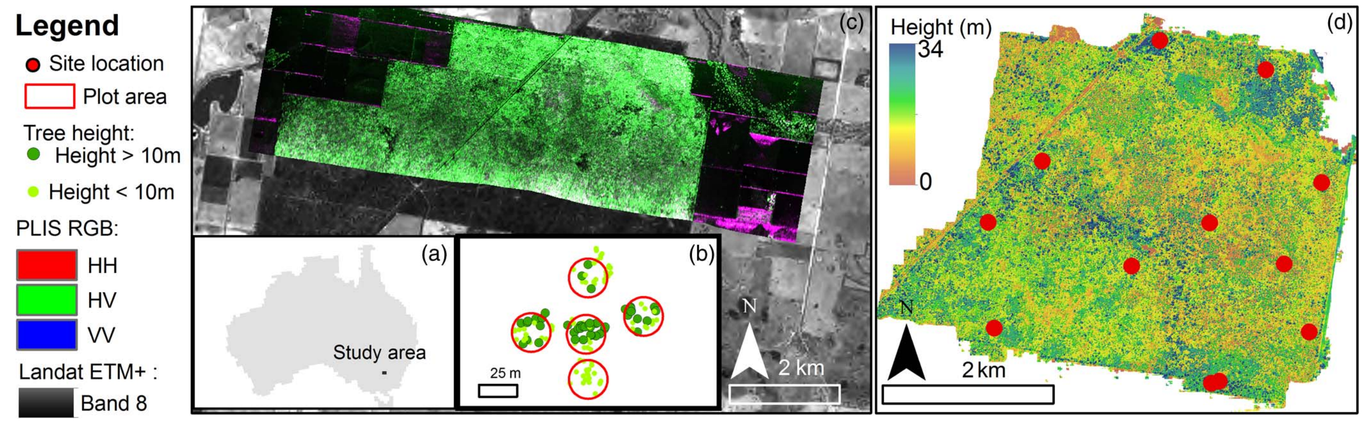

Fig. 1. (a) Study-area location, (b) together with a field sampling site and examples of the airborne data derived from PLIS (C—Backscatter), and ALS Q560 (D—Canopy height model) sensors. The two most South–East sites appear as overlapping due to map scaling.

this study being focused on the Polarimetric L-band Imaging synthetic aperture radar (PLIS) and the Riegl Airborne Laser Scanner (ALS) Q560 [11].

The PLIS is a fully polarimetric sensor with a frequency of 1.26 GHz and tunable bandwidth. Its two antennas illuminate the ground on either side of the aircraft at incidence angles varying from 15° to 45° across the swath. Using a 30-MHz bandwidth, the single-look slant-range resolution is around 6 m. The azimuth resolution is around 0.8 m. More information about the PLIS sensor is found in [12]. The radar sensor was flown nine times between September 5, 2011, and September 23, 2011. With the flights being at an altitude of 3000 m, the average ground swath was 2200 m on each side of the flight line. PLIS polarimetric calibration was accomplished using passive radar calibrators (PRC) and distributed targets [13] with polarimetric calibrated data showing a mean ratio of the copolarized channels of 1 dB and a mean phase difference of 3° to 6° depending on the antenna. After radiometric calibration, the mean difference between the observed and the theoretical PRC cross section was 0.9 (± 0.8) dB.

The ALS Q560 (240 kHz) was flown over the forest area on September 6, 2011, at an altitude of approximately 300 m AGL. The system recorded all echo pulses within a small footprint ($\sim$15 cm) up to a maximum scan angle of $\pm 22.5^\circ$. The lidar sensor was flown from two different directions (N–S and E–W) with a 50% swath overlap that resulted in the same area of the ground being covered four times. An average first-return pulse density of 40 $\mathrm{p} \cdot \mathrm{m}^{-2}$ was obtained after combining all flight lines except for the outer boundaries where the point density was lower. The Riegl software package RiAnalyze was used to extract discrete returns from the raw lidar data. These returns were combined with the navigation data to yield geo-referenced point clouds. Accuracies of this procedure were approximately 0.4 m horizontally and 0.15 m vertically, with higher accuracies within individual scans. Lidar-point-cloud data were classified into ground and nonground returns, with all nonground returns being considered vegetation since no man-made features are located within the forest perimeter.

An on-ground biometric survey was conducted on 60 circular plots (500 m^2 each) clustered in 12 sites (Fig. 1) concurrently with the airborne acquisitions. The selection of the site centers was based on a random sample grid overlaid on a panchromatic Landsat ETM satellite imagery. From the random sample grid, approximately 50 locations were initially selected to represent a variety of forest canopy covers. Before the field campaign, these locations were surveyed to select those locations representative for the range of forest structure conditions encountered in the Gillenbah forest. A cluster site consisted of a center plot with four surrounding plots whose centers were spaced at approximately 35 m in the cardinal directions. The location, circumference, and height of all trees (dead or alive) with a diameter at breast height (dbh) greater than 5 cm were recorded, whereas smaller trees were counted and their average height estimated. In total, 2731 trees were measured for dbh, and the tree height was recorded for 2099 of them. Species-specific allometric equations relating dbh to height were developed and used to estimate the height of the remaining trees. Information on grass cover and average height was recorded from ten additional sparsely vegetated plots. The total above-ground biomass (AGB) and biomass components (leaves, branches, and stem wood) were estimated for each tree using previously defined species-specific allometric equations [14], [15]. The values were subsequently aggregated to plot level. The total AGB for individual plots varied between 1.5 and 179.5 $\mathrm{t} \cdot \mathrm{ha}^{-1}$, with 90% of them being below 100 $\mathrm{t} \cdot \mathrm{ha}^{-1}$. The mean biomass for the 60 forest plots was 60.9 $\mathrm{t} \cdot \mathrm{ha}^{-1}$ with a standard deviation of ± 39.4 $\mathrm{t\,ha}^{-1}$. The mean plot height was 7.2 $\pm$ 2.5 m. Individual tree height varied between 2 and 32.5 m, with the 90th height percentile being 10.5 m for trees over 5-cm dbh. One should notice that ground reference data were collected between September 5, 2011, and September 20, 2011, the same period as for the airborne flights.

III. Methods

Multiple-linear-regression models (1) were developed to predict the total AGB from lidar measurements. Over 65 grid metrics were produced from lidar-point-cloud data at 5-m spatial resolution: 1) canopy closure at 1-, 2-, 4-, 6-, 8-, 10-, and 12-m height, 2) canopy closure and forest density for specific strata (i.e., 1–4 m, 1–6 m, 1–8 m, 1–10 m, 1–12 m, 1–16 m, 1–24 m, 2–4 m, 2–6 m,. . ., 8–16 m, 8–24 m), and 3) overall metrics (i.e., maximum height, canopy surface area, and volume under the canopy surface). Canopy closure metrics were defined as the proportion of first returns over a specific height threshold. Strata-specific canopy closure and forest density metrics were defined as the proportion of first returns and, respectively, all returns falling within specific height thresholds. Each metric was aggregated at plot level and correlated with ground-based plot biomass estimates to select the best AGB predictor variables. The aim was to select one predictor variable corresponding to each forest strata (i.e., overstory and understory) and a general descriptor of the entire plot. The selected lidar-based predictor variables were subsequently used within multiple-linear-regression analysis to estimate the biomass level. Arcsine and log transformations were used to normalize the distribution of the lidar-based grid metrics and the field-based biomass estimates, respectively.

Regression models were also developed for biomass retrieval from SAR backscatter data. Although regression-based relationships derived for specific data sets are not easily transferable, they were preferred to directly compare radar- and lidar-based biomass-retrieval error. The regression models were parameterized using one, two, or three polarizations (2)–(4) to take full advantage of the information provided by the entire scattering matrix measured by the PLIS sensor. Model parameterization was performed using 60% of the sample data, with the remaining 40% retained for validation. The calibration/validation process was repeated 25 times by randomly dividing the data set between training and validation samples to allow a robust estimation of model errors. The root mean squared error (RMSE) and relative RMSE (ratio between RMSE and mean biomass), the model coefficient of determination (R^2), the correlation coefficient between observed and predicted values (r), and the estimation bias were used to evaluate the biomass-retrieval error. In addition, the relative error (RE) was computed for each validation sample and averaged by biomass intervals (5).

$$\mathrm{Log}(AGB) = a + b^{*}asin(Lgm_1) + c^{*}asin(Lgm_2) + d^{*}asin(Lgm_3) \tag{1}$$

$$\mathrm{Log}(AGB) = a + b^{*}\sigma_{xy} \tag{2}$$

$$\mathrm{Log}(AGB) = a + b^{*}\sigma_{xy} + c^{*}\sigma_{yx} \tag{3}$$

$$\mathrm{Log}(AGB) = a + b^{*}\sigma_{\mathrm{xy}} + c^{*}\sigma_{\mathrm{yx}} + d^{*}\sigma_{\mathrm{yy}} \tag{4}$$

$$RE = 100^{*}|AGB_{\mathrm{observed}} - AGB_{\mathrm{predicted}}|/AGB_{\mathrm{observed}} \tag{5}$$

a, b, c, d	model coefficients
Lgm_x	lidar metrics for different strata (see Section IV)
σ_{xy}	backscatter coefficient for xy transmit/receive polarization (dB)
$\mathrm{Log}(AGB)$	natural logarithm of AGB.

The variability of the data explained solely by each predictor term (conditional R^2) was estimated by comparing the fit of the full model (1) and the model excluding the predictor term. The synergy between lidar and radar metrics was tested by adding radar metrics to the multiple-regression model (1) and assessing the improvement of the new model (6) performance based on differences in the Akaike's information criterion (AIC) (Log-likelihood test) and R^2. In addition, a regression model containing only the best correlated metrics (i.e., radar and lidar) with biomass was tested (7). Models multicollinearity was evaluated by examining the tolerance value for each predictor variable. Tolerance is often expressed as the variance inflation factor

TABLE I
SUMMARY OF LINEAR REGRESSION OF AGB AS A FUNCTION OF LIDAR AND RADAR METRICS

Sensor	R^2_{adj}	a	b (Beta)	c (Beta)	d (Beta)	VIF (a;b;c)
lidar	0.871	0.06	-0.95* (-0.2)	2.18* (0.5)	4.57* (0.8)	2.3;1.3;2.0
σ_{HH}	0.544	5.96	0.19* (0.7)	N/A	N/A	N/A
σ_{VV}	0.469	7.35	0.26* (0.7)	N/A	N/A	N/A
σ_{HV}	0.638	7.85	0.21* (0.8)	N/A	N/A	N/A
σ_{VH}	0.644	7.72	0.21* (0.8)	N/A	N/A	N/A
σ_{HH} & σ_{HV}	0.633	7.67	0.03 (0.1)	0.19* (0.7)	N/A	N/A
σ_{HH} & σ_{VV}	0.549	6.58	0.14* (0.6)	0.08 (0.2)	N/A	2.5
σ_{HH} & σ_{HV} & σ_{VV}	0.625	7.63	0.03 (0.1)	0.19* (0.7)	-0.009 (-0.02)	4.3;4.4;2.8

(VIF) which is the inverse of the tolerance. VIF values greater than ten suggest strong collinearity.

$$\mathrm{Log}(AGB) = a + b^{*}asin(Lgm_1) + c^{*}asin(Lgm_2) + d^{*}asin(Lgm_3) + e^{*}\sigma_{xy} \tag{6}$$

$$\mathrm{Log}(AGB) = a + b^{*}arcsine(Lgm_3) + c^{*}\sigma_{xy}. \tag{7}$$

IV. Results and Discussion

Strong correlations ($r > 0.85$, $p < 0.05$) were observed between lidar grid metrics and field-estimated biomass. Although the correlation coefficient varied depending on the sample plots included in the analysis, all values were similar and the best related lidar grid metrics were usually either the same or of the same type (e.g., density and cover metrics). Such small variations are not unusual since different grid metrics are correlated (i.e., vegetation densities for different strata, vegetation density and cover for the same strata, etc.). The selected lidar metrics for biomass retrieval were the following: canopy closure (i.e., Lgm_1—proportion of first returns for 6–8-m strata), vegetation density (i.e., Lgm_2—proportion of all returns for 1–12-m strata), and the volume under forest canopy (i.e., Lgm_3). Most of the variability in forest biomass was explained by Lgm_3 (31%) followed by Lgm_2 (19%). Although Lgm_1 explained less than 2% of biomass variability, it added statistically significant information to the regression model.

Table I shows linear-regression results for the lidar (September 6, 2011) and radar (September 21, 2011—best observed relationships with biomass) data sets. The table also includes the beta standardized regression coefficients (Beta) which can be used to compare the relative strength of the various predictors included in the model, as well as the sign of the relationships between AGB and the lidar/radar metrics. The ALS data performed better when compared with high-resolution fully polarimetric L-band data with significantly higher R^2 being obtained for lidar models. For the radar data, cross-polarized channels (i.e., HV and VH) showed better relationships with biomass explaining up to 75% of its variability. Multiple radar regression models (i.e., including two or three polarizations) did not significantly improve the radar/AGB relationship. Metrics obtained from radar data were essentially redundant when added to a lidar-based model despite the use of a very high-resolution L-band airborne sensor over forests characterized by biomass levels well within radar sensitivity interval (0–100 $\mathrm{t \cdot ha^{-1}}$). In this respect, these findings do not differ from those of [6]–[8] when considering the entire biomass range. All models were statistically significant ($p < 0.05$), with the lidar/radar metrics included in the model being significant except for the multiple radar regression models. For such models, only one metric (i.e., cross-polarized backscatter) was significant, with the remaining one adding little to the general relationship (i.e., low beta coefficients). No evidence of multicollinearity was observed (i.e., $VIF \ll 10$) for either lidar or radar only models.

Previous studies showed that lidar is the best single sensor for estimating biomass levels, with lidar-based metrics producing the most accurate predictive models and having estimation errors varying between 26 and 33.9 $\mathrm{t \cdot ha^{-1}}$[7], [8] for coniferous pine forests. Models using radar-only metrics (i.e., backscatter and/or interferometric height) showed much lower accuracies with RMSE values varying between 52.5 and 57.5 $\mathrm{t \cdot ha^{-1}}$. For our study area, both lidar and radar data provided higher precision for biomass retrieval when compared with previous studies (Fig. 2—average values for the selected error metrics obtained after randomly splitting the ground sample plots between calibration and validation data sets). The RMSE at plot level varied between 26 and 36 $\mathrm{t \cdot ha^{-1}}$ for radar-based models, with the lowest value being observed for cross-polarized channels (Fig. 2 top panel). In percentage, this translates to 60% to 75% error when compared with the average retrieved biomass. For lidar data, an RMSE as low as 17 $\mathrm{t \cdot ha^{-1}}$ (28% relative error) was obtained at plot level, suggesting that lidar-based estimates are twice as accurate (overall) when compared with equivalent high-spatial-resolution-radar-based estimates. Such improvements, with respect to previous studies, could be partly the result of the high point density of the lidar (i.e., 40 $\mathrm{p \cdot m^{-2}}$) and radar data set spatial resolution (i.e., 50 looks at plot level), and the generally lower biomass levels found in the study area. Another factor that could influence the biomass estimation precision in earlier studies is the time lag between data set collection, as new growth is not balanced by stem mortality [7].

The coefficient of determination (R^2) of the modeled radar/lidar and biomass relationships showed relatively high values for both sensor types (Fig. 2 middle panel). However, such high R^2 values did not translate into similar accuracies for the predicted biomass: The correlation coefficient (r) between observed and predicted biomass was significantly lower for radar-based estimates (0.5) when compared with lidar-based estimates (0.9). Such differences imply that sample selection affects the predictive power of the models, i.e., models fitted to the training data set lose their predictive power when applied to independent validation samples. For lidar data, such differences were minimal ($R^2 = 0.88$ and $r = 0.9$). Finally, the estimation bias was similar between the two sensor types when looking at the results for the most sensitive cross-polarized SAR channels (Fig. 2 bottom panel).

The relative error by biomass interval is shown in Fig. 3. Although this error metric suffers from instability when approach-

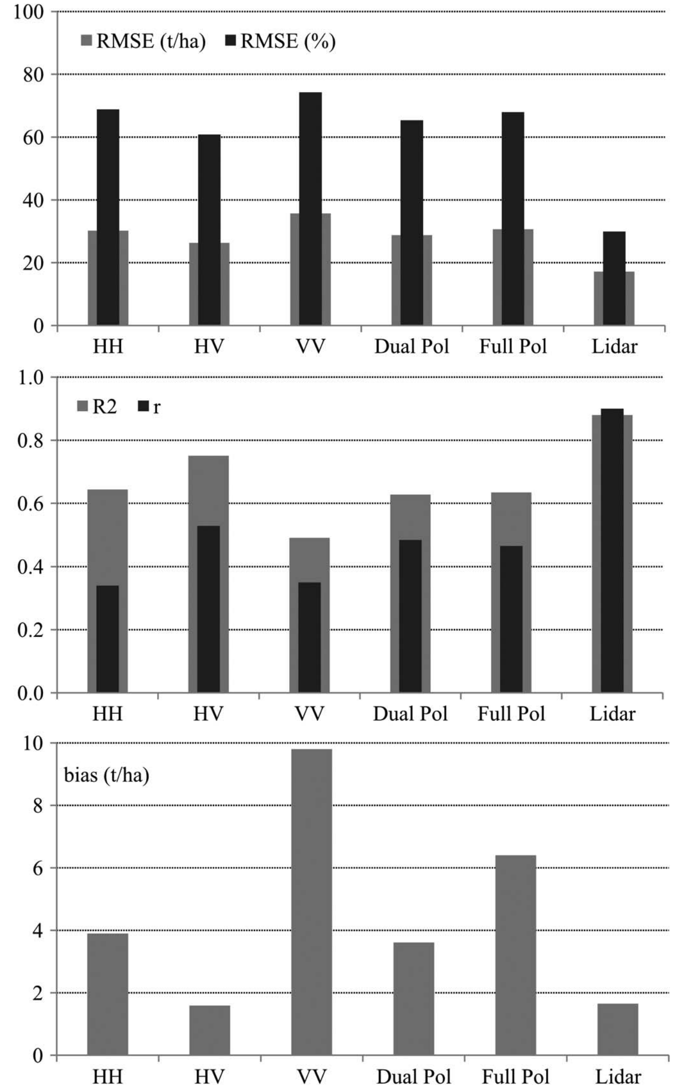

Fig. 2. Model dependent average error metrics (over 25 iterations). (Top panel) RMSE and relative RMSE. (Middle panel) Model coefficient of determination (R^2) and the correlation coefficient (r) between predicted and observed biomass values. (Bottom panel) Bias.

ing zero biomass values (i.e., as the denominator approaches zero, the relative error approaches infinity), its use is valuable when assessing retrieval errors by intervals. For example, an absolute estimation error of 5 $\mathrm{t \cdot ha^{-1}}$ could be considered acceptable for higher biomass intervals (e.g., 50–100 $\mathrm{t \cdot ha^{-1}}$) but would represent a significant deviation from the true value at lower biomass intervals (e.g., 0–10 $\mathrm{t \cdot ha^{-1}}$). The highest estimation error was always associated with the lowest biomass interval (0–10 $\mathrm{t \cdot ha^{-1}}$) for both sensor types, although the magnitude was different. Errors up to 200% were recorded for radar-based biomass retrieval whereas for lidar-based retrieval the errors were as low as 50%. The errors decreased significantly with increasing biomass for intervals below the L-band saturation point (100 $\mathrm{t \cdot ha^{-1}}$), after which the estimation increased for radar-based retrieval. In contrast, lidar data provided much more consistent estimation errors for biomass levels above 10 $\mathrm{t \cdot ha^{-1}}$. However, the most interesting result was the relatively small difference in estimation error between the two sensor types for the 30–100 $\mathrm{t \cdot ha^{-1}}$ biomass range. On the average, radar estimation error for this biomass range was

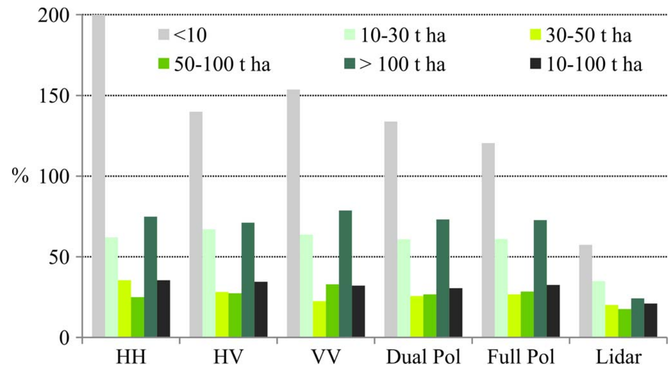

Fig. 3. Relative estimation error (RE) by biomass intervals.

TABLE II
COMBINED LIDAR–RADAR MODELS

Model	AIC	p-value	R^2	VIF (a;b;c;d)
Lidar (eq. 1)	-78.39		0.911	2.3;1.3;2.0
+ HH	-76.53	0.70	0.912	2.3;3.6;2.1;4.1
+ HV	-76.86	0.49	0.913	2.3;2.0;2.3;2.8
+ VV	-76.43	0.85	0.912	2.3;2.5;2.1;2.2

only 9% higher when compared with lidar data, suggesting that at biomass levels below the radar saturation point the retrieval error of the two sensor types is similar. When comparing the entire 10–100 $\text{t} \cdot \text{ha}^{-1}$ biomass range, the difference in the error between radar- and lidar-based biomass retrievals increased from 24% (lidar data) to around 40% (radar data).

Table II shows lidar-model improvement when adding radar-based metrics. Selection of the best predictive model was based on the lowest AIC value [16]. The p-values (log-likelihood test) show whether radar metrics would add statistically significant information to the lidar model. None of the radar metrics significantly improved the model performance, suggesting that radar metrics fail to explain further variability than that already accounted for by lidar metrics. However, when only one lidar metric was used (e.g., total volume under forest canopy), adding radar metrics improved the model performance with HH polarization providing the highest improvement (R^2 increased from 0.72 to 0.84 and AIC decreased from -34 to -56). This suggests that radar data have useful information on forest structure, but this information is not better than what could be obtained by combining different lidar metrics. One should notice that no evidence of model multicollinearity was observed for any of the combined lidar–radar models (i.e., $VIF \ll 10$).

V. CONCLUSION

This letter has analyzed the sensitivity and the estimation error when retrieving plot-level forest biomass from two types of active sensors: fully polarized L-band radar and small footprint airborne lidar. A direct comparison has been carried out using concurrently acquired field and remote-sensing data of similar spatial resolution and over biomass intervals within the sensitivity range of both sensor types. The synergy between the two sensors has also been tested while the estimation errors have been presented by biomass intervals. Overall, biomass retrieval was more accurately estimated from lidar data with both RMSE and the correlation between predicted and observed values being almost twice as higher when compared with radar estimates. However, for the 30–100-$\text{t} \cdot \text{ha}^{-1}$ biomass interval, the difference in relative retrieval error between the two sensors was much smaller (i.e., 9%). Jointly using lidar and radar data did not provide any further improvement to the biomass-retrieval error.

Which sensor is more appropriate for biomass retrieval ultimately depends on the desired accuracy, spatial extent, temporal frame, and cost constraints. For forest-management purposes, lidar data constitute the method of choice given that it provides the most accurate estimates for all biomass intervals. Conversely, L-band radar data may offer relatively accurate estimates for some biomass intervals, which could be valuable for large-area and frequent monitoring studies.

REFERENCES

[1] R. Nelson, R. Swift, and W. Krabill, "Using airborne lasers to estimate forest canopy and stand characteristics," *J. Forest.*, vol. 86, no. 10, pp. 31–38, Oct. 1988.
[2] M. Nilsson, "Estimation of tree heights and stand volume using an airborne LiDAR system," *Remote Sens. Environ.*, vol. 56, no. 1, pp. 1–7, Apr. 1996.
[3] E. J. Rignot, J. Way, C. Williams, and L. Viereck, "Radar estimates of aboveground biomass in boreal forests of interior Alaska," *IEEE Trans. Geosci. Remote Sens.*, vol. 32, no. 5, pp. 1117–1124, Sep. 1994.
[4] G. Sandberg, L. M. H. Ulander, J. E. S. Fransson, J. Holmgren, and T. L. Toan, "L- and P-band backscatter intensity for biomass retrieval in hemiboreal forest," *Remote Sens. Environ.*, vol. 115, no. 11, pp. 2874–2886, Nov. 2011.
[5] M. Santoro, L. Eriksson, J. Askne, and C. Schmullius, "Assessment of stand-wise stem volume retrieval in boreal forest from JERS-1 L-band SAR backscatter," *Int. J. Remote Sens.*, vol. 27, no. 16, pp. 3425–3454, Aug. 2006.
[6] P. Hyde, R. Dubayah, W. Walker, J. B. Blair, M. Hofton, and C. Hunsaker, "Mapping forest structure for wildlife habitat analysis using multi-sensor (LiDAR, SAR/InSAR, ETM+, quickbird) synergy," *Remote Sens. Environ.*, vol. 102, no. 1/2, pp. 63–73, May 2006.
[7] P. Hyde, R. Nelson, D. Kimes, and E. Levine, "Exploring LiDAR–RaDAR synergy—Predicting aboveground biomass in a southwestern ponderosa pine forest using LiDAR, SAR and InSAR," *Remote Sens. Environ.*, vol. 106, no. 1, pp. 28–38, Jan. 2007.
[8] R. F. Nelson, P. Hyde, P. Johnson, B. Emessiene, M. L. Imhoff, R. Campbell, and W. Edwards, "Investigating RaDAR–LiDAR synergy in a North Carolina pine forest," *Remote Sens. Environ.*, vol. 110, no. 1, pp. 98–108, Sep. 2007.
[9] J. O. Sexton, T. Bax, P. Siqueira, J. J. Swenson, and S. Hensley, "A comparison of lidar, radar, and field measurements of canopy height in pine and hardwood forests of southeastern North America," *Forest Ecol. Manag.*, vol. 257, no. 3, pp. 1136–1147, Feb. 2009.
[10] M. C. Dobson, L. Pierce, K. Sarabandi, F. T. Ulaby, and T. Sharik, "Preliminary analysis of ERS-1 SAR for forest ecosystem studies," *IEEE Trans. Geosci. Remote Sens.*, vol. 30, no. 2, pp. 203–211, Mar. 1992.
[11] C. Hug, A. Ullrich, and A. Grimm, "LITEMAPPER-5600—A waveform digitising lidar terrain and vegetation mapping system," in *Proc. Int. Arch. Photogramm. Remote Sens. Spatial Inf. Sci*, 2004, vol. 36, pp. 24–29.
[12] D. Gray, Y. Ruiting, H. Yardley, R. Panciera, J. Walker, J. Hacker, A. McGrath, B. Bates, and N. Stacy, "PLIS : An airborne polarimetric L-band interferometric synthetic aperture radar," in *Proc. Int. APSAR Conf.*, Seoul, Korea, 2011, pp. 845–848.
[13] A. S. Goh, M. Preiss, D. A. Gray, and N. J. S. Stacy, "Comparison of parameter estimation accuracy of distributed-target polarimetric calibration techniques," in *Proc. IEEE Geosci. Remote Sens. Symp.*, Jul. 2007, pp. 4175–4178.
[14] W. H. Burrows, M. B. Hoffman, J. F. Compton, and P. V. Back, "Allometric relationships and community biomass stocks in white Cypress Pine (Callitris Glaucophylla) and associated Eucalpyts of the Carnarvon area, central Queensland," Australian Greenhouse Office, Canberra, Australia, Tech. Rep. No.33, 2001.
[15] S. D. Hamilton and G. Brodie, "Allometric relationships for estimating biomass in grey box (Eucalyptus Microcarpa)," *Australian Forestry*, vol. 68, no. 4, pp. 267–273, Jan. 2005.
[16] H. Akaike, "A new look at the statistical model identification," *IEEE Trans. Autom. Control*, vol. AC-19, no. 6, pp. 716–723, Dec. 1974.